Waters Symposium

edited by
C. W. Gardner
ChemImage Corporation
Pittsburgh, PA 15208

The Impact of Array Detectors on Raman Spectroscopy

Stephen C. Denson, Carolyn J. S. Pommier, and M. Bonner Denton*
Department of Chemistry, University of Arizona, Tucson, AZ 85721; **mbdenton@u.arizona.edu*

Sir C. V. Raman discovered Raman scattering in 1928. Owing to the relatively low intensity of Raman scattering, with only low-intensity sources and relatively insensitive detectors initially available, only highly concentrated samples could be routinely analyzed. Today, many major advances in lasers, advanced optical components, such as volume-phase holographic filters and high performance scientific array detectors, have made modern Raman instrumentation highly sensitive and capable of routine analyses. This article was written as a review of a presentation given at a Waters Symposium on Raman spectroscopy by one of the authors: M. Bonner Denton *(1).* While the focus of the article is the impact of array detectors in the field of Raman spectroscopy, most aspects of array detectors presented are applicable to all low-light-level spectroscopic techniques.

Detector Characteristics

Before discussing the different types of detectors used in Raman spectroscopy, a brief section defining various detector characteristics is necessary.

Quantum Efficiency

Quantum efficiency (QE) is the percentage of incoming photons that are converted into charge by the detector. As the wavelength of the incident photons changes, the response of the detector also changes. The physical composition of a given detector determines how well or poorly the detector responds to different wavelengths. The QE is a critical factor in the determination of whether or not a detector is suitable for a given experiment *(2).*

Full Well Capacity

The full well capacity (FWC) only applies to integrating detectors and is the maximum quantity of charge a detector element can store during one integration. An integrating detector will continue to accrue and store charge as long as it is being exposed to photons, until it reaches the FWC. At this point no further charge can be accepted and on some integrating detectors other detrimental effects, including charge spreading into adjacent pixels (blooming), can occur.

Charge-Transfer Efficiency

Charge-transfer efficiency (CTE) is the measure of how well charge packets are transferred from one site to the next. In charge-coupled devices (CCDs) large numbers of transfers are required and a CTE of 99.999%, or better, is desired.

Dark Current

Dark current is a signal generated spontaneously by a detector. Dark current is predominantly due to thermally produced charge and therefore most detectors are cooled to reduce the dark current *(3).* In most focal-plane array detectors dark current is reduced by a factor of two for every seven to eight degrees Celsius the detector is cooled until further cooling results in detrimental effects on other detector parameters. Silicon CCDs, for example, can be cooled to approximately −100 °C to −140 °C, but at colder temperatures the CTE begins to deteriorate *(3).* A significant dark current will limit the potential exposure time during an experiment because the dark current alone will eventually cause the detector to reach saturation (FWC).

Shot Noise

Shot noise is a result of the random nature of the arrival of photons and is given as the square root of the total signal. Shot noise can originate from the sample, from background sources, or from fluorescence of trace constituents and can be a significant, if not overwhelming, contribution to the total noise of an experiment *(4).*

Read Noise

Read noise is inherent in the electronics that amplify and process the signal from the detector and is often attributed to the entire detection system. Read noise is independent of integration time and signal amplitude. When the signal amplitude is high the read noise is normally not significant, but the signal-to-noise ratio (S/N) can be limited when the signal intensity is low. The S/N must be at least three (signal level is three times greater than the standard deviation of the noise) for a signal to be considered analytically detectable. If the experiment is easily reproduced multiple reads can be averaged to reduce the read noise by the square root of the number of reads averaged.

Single-Channel Detectors

Photomultiplier Tubes

The photomultiplier tube (PMT) was commonly used as a detector for Raman spectroscopy before modern array detectors became available. PMTs are termed single-channel detectors because they have only one light sensitive area. A PMT has a photosensitive cathode and a collection anode separated by several other electrodes, called dynodes. The dynodes serve to provide signal multiplication or gain. A photon incident on the photocathode can cause a photoelectron to be released. By properly biasing the potentials of the dynodes the photoelectron is drawn to the first dynode with enough acceleration that it “knocks out” two to five secondary electrons upon impact. Each secondary electron is guided to the next dynode where more secondary electrons are released until the anode is reached and the resulting current can be measured. This cascade effect is capable of providing a signal gain of 10^4 to 10^6 or more *(5, 6).*

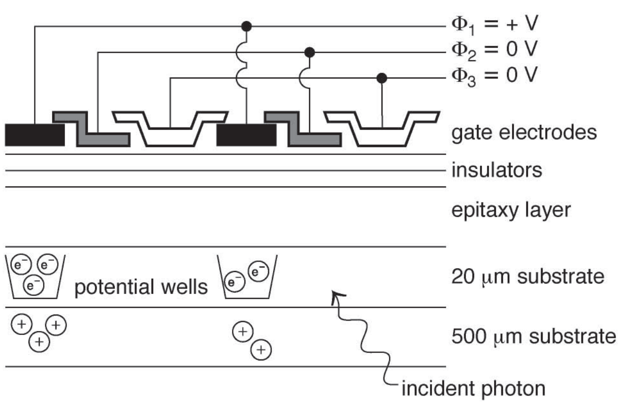

Figure 1. Cross-sectional view of a three-phase CCD architecture (three gates per pixel). Setting one gate at a positive voltage creates a potential well where electrons are collected.

To acquire a full spectrum with a single-channel detector, a monochromator must be set to a narrow wavelength range and the monochromator must be scanned through the wavelength range of interest. Data must be collected at each monochromator step. This sequential scanning is extremely time consuming and also requires that all experimental parameters, except wavelength, are constant during the scan. Fluctuations in the source intensity can easily lead to spurious results and dynamic systems are not easily studied because the spectrum can change in the time required to scan multiple wavelengths. In addition to being limited to a single resolution element, PMTs also exhibit high dark current and relatively poor sensitivity (low QE), particularly in the red and near-infrared red regions.

Photodiodes

Silicon photodiodes absorb incident photons in the p–n junction of a reversed biased diode and create electron–hole pairs. The change in potential across the p–n junction can be measured as a function of the number of charge carriers produced by photons *(5)*. Photodiodes are typically less sensitive than PMTs because of the large internal gain of the PMT, but the simplicity, excellent linearity, and wide spectroscopic response of photodiodes make them incredibly useful for experiments where the light level is high. The small size of photodiodes, 25 to 50 µm, allows for a collection of photodiodes to be connected to form an array detector.

Array Detectors

An array, or multichannel, detector has many resolution elements (separate light sensitive areas) typically arranged in either a linear format or a rectangular, two-dimensional format. Systems incorporating multichannel detectors will nearly always consist of a spectrograph that disperses different wavelengths across the detector allowing simultaneous detection of multiple wavelengths. The various multichannel detectors that have been used and are still being used for Raman spectroscopy will be discussed and compared in the following sections. Other array detectors no longer widely used for Raman spectroscopy, including image dissectors, vidicons, intensified target vidicons, and more, are discussed elsewhere *(7)*.

Photographic Emulsion

The first "multichannel" detector was the photographic emulsion. Undeveloped film was placed at the focal plane of a spectrograph where it could collect an entire spectrum in one exposure. A photographic emulsion is simple to expose, inexpensive, and sensitive to light levels as low as 10 to 100 photons *(5, 8)*. Unfortunately, film has a long development time, a low dynamic range, and is difficult to use for quantitative analyses. As a result photographic emulsions have been replaced with electronic transducers.

Photodiode Arrays

Photodiode arrays (PDAs) consist of arrays of silicon photodiodes mounted on a silicon support. Linear formats, with typical array sizes between 256 and 4096 photodiodes, are available. The PDA is positioned across the focal plane of a spectrograph so that each photodiode receives a narrow wavelength range. Incident radiation creates electron–hole pairs that discharge a capacitor in each photodiode. The total quantity of current required to recharge the capacitor to its nominal level after an exposure determines the quantity of light that struck that element of the photodiode.

The QE of a PDA is dependent on the photoresponse of silicon. At 550 nm the QE is the highest at approximately 70% and from 200 to 900 nm typically stays above 20%. Farther into the infrared the photoresponse of silicon drops sharply, 1% or less at 1100 nm, because the incident photons lack sufficient energy to create an electron–hole pair. Overall the QE of a PDA is superior to that of a PMT, but a PMT is generally more sensitive than a PDA because of the internal gain of a PMT.

Compared to other silicon-based multichannel detectors used for Raman spectroscopy, PDAs often have a high dark current. A PDA cooled to −20 °C had a dark current of 40 electrons per second *(9)*. As with most detectors the dark current can be reduced to insignificance with further cooling. The biggest limitation of PDAs is the read noise, which can be between 1700 and 3750 electrons per pixel *(10)*, compared to 2 to 20 electrons per pixel in CCDs *(3)*. Initially, PDAs offered vastly improved acquisition time and ease of quantitation over photographic emulsions, but today other silicon-based transducers generally out-perform PDAs. Thus PDAs are a less popular choice for Raman spectroscopy.

Charge-Coupled Devices

General Operation

The concept for CCDs was invented in 1969 by Willard Boyle and George Smith of Bell Laboratories *(11)*. CCDs became commercially available in 1973 and are now found on spectrometers in teaching laboratories *(12)* and CCDs are one of the most commonly used detectors in many spectroscopic applications, including Raman spectroscopy *(13, 14)*. More detailed histories of CCD array detectors are presented by Sims *(15)* and Janesick *(16)*.

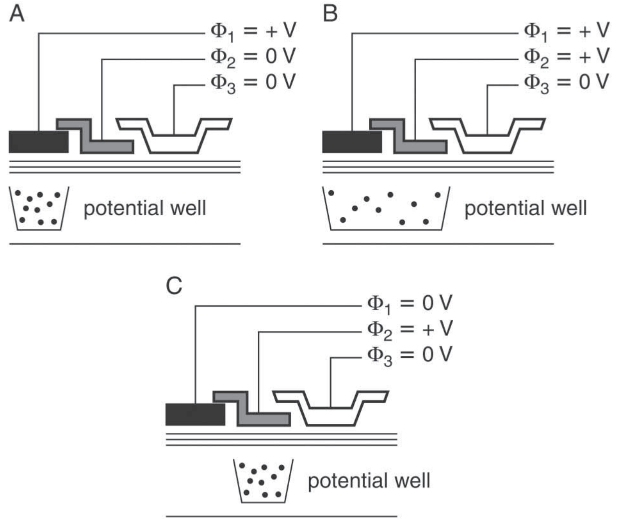

Figure 2. Charge-transfer operation in CCDs: (A) Electrons are collected under the positively biased gate. (B) The potential of the next gate is raised to the same level as the first and the electrons spread out between the two gates. (C) The potential on the first gate is set to zero and the electrons are then exclusively under the second gate. This process is repeated for the third gate and then the first gate of the next pixel and so on.

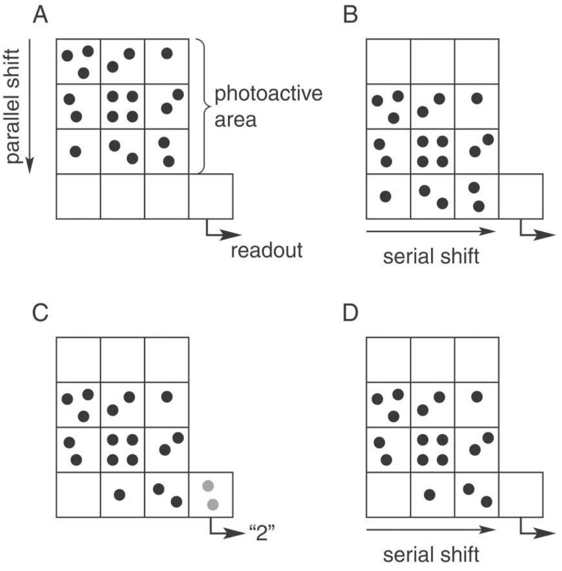

Figure 3. Charge readout of a CCD: (A) Charge is collected in photoactive areas of CCD. (B) Parallel shift transfers all rows of charge down one row towards serial register. (C) Serial shift moves charge in the serial register only toward the readout and the charge is quantified. (D) Reading clears charge in readout node. Serial shift is repeated until the serial register is cleared at which point another parallel shift occurs. This process continues until the full device is read.

CCDs are made up of a one or two-dimensional array of resolution elements, called pixels, mounted on a silicon chip. Each pixel has several metal oxide semiconductor electrodes, called gates (Figure 1). Charge can be transferred between pixels by the following mechanism. Initially one of the gates is held at a positive potential and as incident photons create electron–hole pairs in the silicon the electrons are attracted to, and stored in, a potential well under this gate (Figure 2A). When the exposure is complete the potential on the next gate is raised to the same positive value on the first gate and the electrons are then spread out evenly between the two gates (Figure 2B). The potential on the first gate is then lowered so all the electrons are shifted (or transferred) under the second gate (Figure 2C).

To read the full device, a parallel shift first occurs, which simultaneously shifts the charge on all of the rows of the CCD down by one row toward an extra row of photo-inactive pixels called the serial register. The charge in the last ("bottom") row of the photoactive area is shifted into the serial register. A serial shift is then initiated, which transfers the electrons on a pixel-by-pixel basis to the readout electronics where the charge is quantified and cleared. Once every pixel on the serial register has been read, another parallel shift occurs and another full row of charge is moved onto the serial register. The process is repeated until the charge on the entire device has been read *(3)* (Figure 3). The output is a sequence of voltages corresponding to the number of electrons collected by the individual pixels.

Array Formats

CCD arrays and pixels are both available in a variety of sizes and formats. The sizes desired depend on many factors including the required resolution, which can be increased with larger array sizes and smaller pixels, the desired readout speed, which is typically faster for smaller arrays, and the cost. Today, Raman spectroscopy normally utilizes rectangular CCD arrays. If the wavelengths are dispersed horizontally across the long axis of the CCD, each pixel on the same vertical axis, or column, will acquire photons of the same wavelength. In dispersive Raman spectroscopy there is typically no need for a second dimension of resolution and all the electrons from the pixels on the same vertical axis (same wavelength) can be summed together prior to readout in a process called binning. Binning reduces the total number of read operations required to readout the complete CCD and results in a decrease in both the read noise and the readout time, but makes "cosmic ray" events harder to eliminate.

Quantum Efficiency

Raman spectroscopy is a low-light level technique and requires highly sensitive detectors to maximize output signals. A CCD offers better QE than most detectors in the ultraviolet, in the visible, and in the near-infrared depending on how the CCD is fabricated. The QE of a CCD is dependent, in part, on the photon penetration depth, or the depth at which incident photons create electron–hole pairs. The photon penetration depth is dependent on the wave-

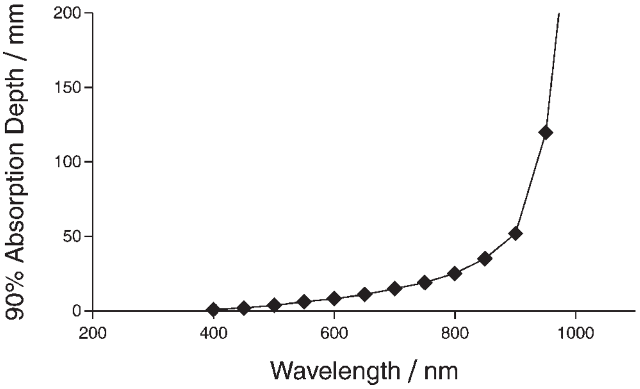

Figure 4. Graph of photon penetration depth versus wavelength. As the wavelength increases the depth at which 90% absorption occurs increases.

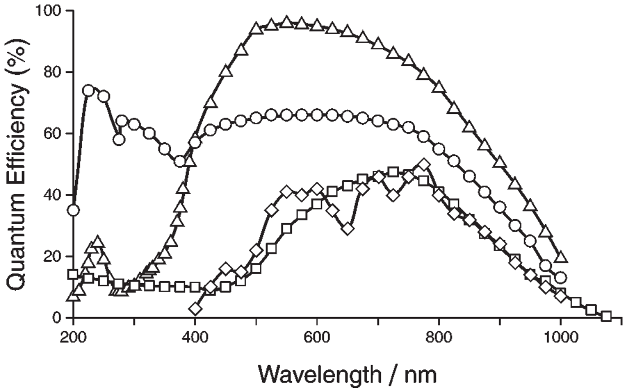

Figure 5. QE curves of various CCDs: (◇) normal frontside-illuminated CCD, (□) frontside-illuminated CCD with a phosphor coating, (△) backside-illuminated CCD with AR coating optimized for the visible, and (○) backside-illuminated CCD with AR coating optimized for the ultraviolet *(25)*.

length of the photons. Ultraviolet photons travel only a short distance before 90% of the photons are converted into electron–hole pairs, but as the wavelength increases the penetration depth increases (Figure 4).

CCDs with an epitaxial layer 10–20 μm thick have poor QE in the near-infrared region because most of the incident photons pass through the epitaxy and never create an electron–hole pair *(3)*. The near-infrared QE of CCDs can be raised through the use of optimized and "thick-epi" devices with epitaxy layers at least 50 μm thick.

The photon penetration depth phenomenon also poses a problem in the ultraviolet region. The ultraviolet photons have such a shallow photon penetration depth that the photons are absorbed in the gate electrodes and electron–hole pairs are never created. The ultraviolet QE of a frontside-illuminated CCD is typically less than a few percent. The gate structure on the front of the CCD is a necessity, but the majority of the substrate on the back of the CCD can be removed and the CCD can be "backside-illuminated". The substrate is typically hundreds of micrometers thick and must be etched away to expose the epitaxy layer. The etching process is costly and leaves the CCD in a very fragile state, but the QE of a backside-illuminated CCD can be greater than 40% in the ultraviolet.

Another method for the improvement of the ultraviolet QE of a CCD is to coat the frontside of the device with a phosphor. The phosphor absorbs photons, then fluoresces at longer wavelengths. The phosphor is chosen such that the emission overlaps with the peak QE of the CCD, typically between 400 and 550 nm. The phosphor is responsive to photons in the ultraviolet region and results in an increase in the wavelength range of the device. Unfortunately, the QE of a phosphor-coated CCD can never be higher than 50%. The emission from the phosphor is isotropic, so half the emitted photons are sent back toward the source of the photons and never reach the CCD. Additionally, there will be a loss in spatial resolution owing to the phosphor's isotropic emission.

CCD QE is also limited by the reflectivity of silicon; however, this can be overcome through the application of an anti-reflection (AR) coating. The gate structure on the front of the CCD (Figure 1) prevents AR coatings from being applied uniformly and effectively, but the back of a backside thinned CCD is level and uniform allowing an even coating to be applied once the substrate has been etched away. The QE of a backside-illuminated, AR-coated CCD can exceed 90%. The QE curves of several different CCD constructions are presented in Figure 5.

Dark Current

Dark current in CCDs is primarily derived from the thermionic emission that occurs in surface defect sites in the silicon, particularly when a gate electrode is energized. The quantity of dark current is related to the temperature of the CCD. For every 8 °C decrease in temperature the dark current drops by approximately 50%. To take advantage of this temperature dependence, CCDs are often cooled thermoelectrically or cryogenically with liquid nitrogen. Thermoelectric coolers can lower the temperature to −30 to −60 °C. At these temperatures the dark current is only a few electrons per pixel per second, but even this level can impose a limit on integration times. If the CD is cooled cryogenically to −100 to −140 °C the dark current is less than one electron per pixel per second. Although a CCD could be cooled further to reduce dark current, the charge-transfer efficiency—the percentage of charge transferred from pixel to pixel—begins to drop, which results in a reduction of the efficiency of the CCD.

Dark current in CCDs also originates from spurious electron generation in extraneous bonds between the epitaxy and insulator layers. The CCD architecture can be modified to operate in multipinned phase (MPP) mode to reduce this effect. A shallow *p* implant is placed under one of the gates in a three- or four-phase CCD architecture—three or four gates per pixel (Figure 6).

The potential energy of that gate is raised and a potential barrier is created even when all of the gates are operated at the same potential. Without this potential barrier the charge collected under any one pixel would spill over into adjacent pixels. During integration all of the gates are biased slightly negative to cause surface inversion. As a result positive charge is attracted to the gates and the most of the electrons generated from surface states are prevented from reaching the potential wells. The barrier implant is not as effective at preventing charge from entering adjacent pixels as a positively biased gate and the FWC is reduced by as much as a factor of two; however, an MPP-mode CCD typically exhibits a dark current 10 to 30 times lower than does a standard CCD. CCDs already exhibit better dark-current behavior than other detectors, but the reduction of dark current allows an MPP-mode CCD to operate at higher temperatures and still achieve the desired low dark current *(3).*

Read Noise and Readout Speed

Most CCDs have lower read noise than other available integrating detectors with 2 to 20 electrons per pixel at the slowest readout rates *(3).* Not only is this read-noise behavior vastly superior to PDAs, but the effective read noise can be further reduced through binning, which is unavailable in PDAs. Most CCDs offer several different readout speeds, but as the readout speed increases the read noise often increases. Another method to increase the readout speed of a CCD is to only read a subarray of the full CCD. If only a limited range of wavelengths is desired or a section of the CCD does not contain any useful information, readout time can be lowered by not reading the extraneous portions of the CCD. These features allow users to choose a compromise between the readout speed and the level of read noise.

"Cosmic Ray" Events

Cosmic ray events (CREs), so termed by astronomers using CCDs, are another source of noise common to silicon-based detectors. When high-energy, background radiation, caused by radioactive decay and random cosmic events, impinge on a light-sensitive area of a CCD a large number of electron–hole pairs are generated. As a result a single pixel will return an abnormally high photon count. Although the camera software can easily remove CREs after readout, this sensitivity to radiation must be considered when a CCD camera is assembled. For example, optical windows often incorporate thorium oxide to give a high refractive index and low dispersion *(17),* but α-particles from the radioactive thorium give rise to a large number of CREs.

Blooming

Blooming is an inherent problem in CCDs and can occur when one pixel, or more, reaches the full well capacity. At this point additional photons incident on the saturated pixel generate more electron–hole pairs and some of the new charge spills over into neighboring pixels. On a two-dimensional array the image would appear to have stripes running away from any bright areas. Blooming is an especially serious problem if both low and high light levels are to be measured simultaneously. The integration time must be sufficient to detect the low-intensity feature, but if the time is too long the high-intensity feature may cause blooming, which could obscure the low-light feature. Blooming can be prevented with special drains on the CCD, but the addition of these drains can decrease the photoactive area available on the CCD and reduces the overall sensitivity of the detector.

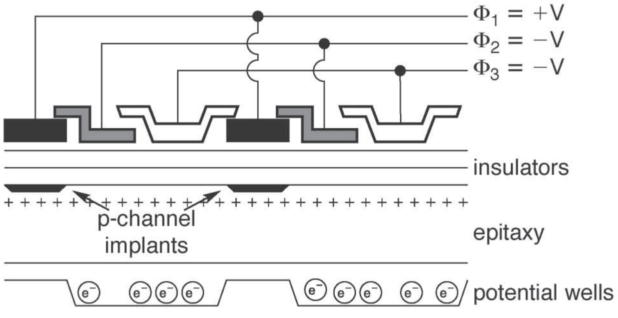

Figure 6. Multiphase pinned (MPP) architecture. During charge integration all gates are biased negatively, but the buried *p*-channel creates a barrier between pixels. Dark current is reduced as a result of the surface inversion created by the negative gates.

Summary of Fluorescence-Free Raman

Modern CCDs offer lower dark current, lower read noise, and better QE than most, if not all, other available detectors. All of these qualities make CCDs excellent choices for detectors in Raman spectroscopy. Because the price of CCDs has decreased substantially most commercial, dispersive Raman spectrometers are now sold with a CCD as the standard detector.

Non-Silicon Array Detectors

Raman spectroscopic studies using excitation sources emitting in the visible region are frequently plagued by fluorescence from the sample or a contaminant within the sample. In many cases the fluorescence is broad and intense enough to completely obscure the Raman signal. The probability of fluorescence can be reduced through the use of a near-infrared or an infrared excitation source so that insufficient energy is imparted to the sample to cause fluorescence. Silicon-based devices can not be used in the infrared beyond 1100 nm because the photons do not have enough energy to create electron–hole pairs in the silicon.

Germanium (Ge) detectors are usually available in linear arrays of 128 or 256 pixels. The small size of the Ge array limits the wavelength coverage and resolution, but the grating in the spectrograph can be rotated to give a different wavelength range and all the spectra can be combined later. Ge detectors can detect wavelengths from 800 to 1600 nm and the QE in this range averages 60% *(18).* In linear Ge detectors each pixel is separately connected and the read noise of Ge devices is substantial. Multiple scans must be acquired and averaged to achieve acceptable S/N *(19, 20).* Ge devices can be cooled with liquid nitrogen to reduce the dark current to allow long integration times, but cooling cryogenically reduces the longest detectable wavelength from 1600 nm to 1450 nm *(21).*

Indium gallium arsenide (InGaAs) detectors were developed to improve upon Ge detectors. InGaAs arrays are linear devices with as many as 512 pixels *(22).* The sensitive

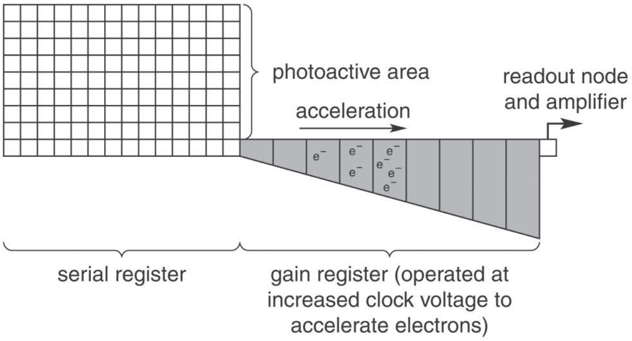

Figure 7. Architecture of a multiplier CCD. A gain register is added between the serial register and readout to provide signal amplification *(24)*. The gain register is operated at an increased clock voltage, which accelerates the electrons during transfer causing multiplication.

region extends from 800 nm to between 1700 nm and 2200 nm depending on the composition of the detector. The QE of InGaAs devices averages 80% *(22),* an improvement over Ge devices. The dark current can be reduced to as little as one electron per pixel per second at cryogenic temperatures *(22),* but as a result the wavelength coverage is reduced. The read noise of InGaAs arrays is still quite significant at 650 electrons per pixel *(22).*

There are several other non-silicon detectors available for Raman spectroscopy. Platinum silicide (PtSi) detectors are available in two-dimensional formats and can detect wavelengths from 1 μm to 5 μm. Unfortunately, PtSi detectors have a QE of only 26% for most of that range. Mercury cadmium telluride (MCT or HgCdTe) detectors hold great potential for use in infrared Raman systems. The QE of an MCT detector is over 60% between 800 and 2500 nm *(23),* the dark current is less than 0.1 electrons per pixel per second, and the read noise is under 10 electrons per pixel per read. Also, MCT arrays are available in two-dimensional formats and allow imaging experiments to be performed in the infrared.

Overall non-silicon detectors are not as efficient as silicon systems. The QE is lower, the read noise is higher, the cost is higher, and the small size of available arrays imposes a limit on the wavelength range than can be simultaneously detected. The non-silicon devices are also sensitive to environmental infrared emissions and must be carefully shielded so that measurements are not ruined by ambient infrared sources (including the inside of the polychromator). Despite these disadvantages non-silicon devices provide promise as a means to work in a nearly fluorescence-free region.

Recent Advances in Array Detectors

Multiplier CCDs

Recently, CCDs have been enhanced by a new method for signal intensification that uses neither phosphor coatings nor microchannel plates *(4).* These “multiplier CCDs” use an on-chip charge-multiplication to provide gain for the output signal. In a normal CCD a full row of charge is first shifted onto the serial register; then the charge is transferred through the serial register to the readout electronics. In a multiplier CCD a gain register is added between the standard serial register and the readout (Figure 7).

The gain register shifts charge in a similar fashion to that of the rest of the CCD, except the gates use much higher than normal clocking potentials: 40–50 V versus 10 V. The larger potential difference results in an electric field that causes a cascade multiplication of the electrons as they are transferred. Each stage of gain may only increase the signal by a small percentage, but over 500 stages this results in a major signal amplification (*24*) (from 100-fold to over 1000-fold amplification).

Apart from the gain, one other advantage of the multiplier CCDs is the potential increase in S/N. The multiplication occurs prior to the readout, so the signal increases dramatically while the read noise remains constant. This benefit only appears for noise generated during or after readout. Any noise introduced before or during the multiplication step will be amplified along with the signal and S/N will remain constant. For a low-light experiment with read noise as the dominant noise source, the increase in the S/N is dramatic. In situations where other noise sources are present and are amplified along with the signal, a multiplier CCD can offer a vastly reduced exposure time.

Multiplier CCDs are being manufactured by at least two companies. Marconi *(24)* and Texas Instruments *(25)* have multiplier chips commercially available in cameras produced by Andor Technology *(26)* and Roper Scientific *(27).*

Hybrid Imaging Technology

Hybrid Imaging Technology (HIT) describes a new type of detector that capitalizes on the advantages of both CCD technology and complementary metal oxide semiconductor (CMOS) technology. Today, CCDs provide the ultimate in sensitivity, but the readout of a typical CCD has a gain of less than one. CMOS imaging arrays are fairly insensitive, but CMOS signal-processing technology is capable of high gain. In HIT the analog readout electronics are incorporated in a CMOS chip allowing multiple copies to be included on a single die. This allows the CCD to be divided into several sections with each section read in a parallel fashion at a reduced speed. Thus, through a combination of the two technologies HIT detectors are simultaneously capable of providing high speed, low noise, high sensitivity, large dynamic range, and low power requirements. HIT devices are currently being developed by Imager Labs *(28).*

The Impact of Array Detectors on Modern Raman Spectroscopy

Array detectors have led to significant breakthroughs in Raman spectroscopy particularly in the reduced acquisition time necessary to collect Raman spectra. In addition, the recent commercialization of Raman libraries now allows unknown chemicals, pharmaceuticals, and polymers to be routinely identified within a matter of minutes, or even seconds. Libraries of gem and mineral spectra are under development to provide a non-destructive alternative for identification of potentially expensive samples. X-ray powder diffraction, the conventional technique for mineral identification, can be both time consuming and destructive *(14).* Raman can also be used quantitatively at low concentrations thanks, in part, to the low noise and high sensitivity afforded by CCD detectors. Linear calibration curves can be generated across five orders of magnitude of concentration and, in a region free of interferences, the detection limit can be less than a part per million *(13).* In addition to the vast improvements in traditional Raman spectroscopy, array detectors have also made several new Raman experiments possible including the collection of simultaneous spectra, ultraviolet Raman, and Raman imaging.

Simultaneous Spectra Collection

Two-dimensional arrays can be used to simultaneously collect full Raman spectra from several different samples. The output of the excitation laser is split and each beam is directed into a different fiber of a fiber optic bundle. Each fiber then illuminates a separate sample and another fiber optic bundle (one bundle per sample) is used to collect the resultant Raman signal. The fibers in this collection bundle are then arranged along the axis of the entrance slit of the spectrograph and the detector acquires Raman spectra with wavelengths dispersed along one axis and different samples separated on the other axis. It is vital that there is no overlap between the spectra. The fiber bundles must be configured very carefully to ensure that a given Raman spectrum does not have superimposed interferences from neighboring spectra.

Fluorescence-Free Raman

Fluorescence can easily limit the effectiveness of Raman spectroscopy. If the sample or a trace-level contaminant fluoresces at the wavelength of a given excitation source it can become difficult or impossible to analyze that sample with that source. A near-infrared sensitive CCD and a near-infrared source reduce the probability of fluorescence, but even using a 785-nm source fluorescence is sometimes an issue. Wavelengths longer than 785 nm can be used, but silicon-based detectors can only detect photons from wavelengths shorter than 1100 nm. The continued development of non-silicon detectors should allow near-infrared and infrared excitation sources to be used and still provide sensitive, two-dimensional array detectors.

Another alternative to using infrared sources to reduce or remove problems from fluorescence exists. At ultraviolet excitation wavelengths, fluorescence is even more likely to occur, but the normal fluorescence emission is shifted to longer wavelengths. If the excitation is sufficiently far in the ultraviolet, a region free of fluorescence interference is left in which Raman scattered light can be collected *(29).* At ultraviolet wavelengths the region of interest for Raman spectroscopy is approximately 20-nm wide. Most fluorescence emission occurs at wavelengths of 260 nm or longer so a laser emitting at 240 nm or shorter is an excellent source for fluorescence-free Raman. There are only a few choices of array detectors capable of ultraviolet detection. An intensified CCD could be used, but only offers 15–20% QE at best *(30)* and would suffer from resolution losses and the high dark current associated with the MCP (*4*). A better choice is a backside-illuminated CCD with an AR coating optimized for the ultraviolet that offers QE of 60–75% from 225 to 300 nm *(31)* (Figure 5).

Currently the primary limitation to ultraviolet Raman is the availability of excitation sources. Frequency-doubled and quadrupled lasers emit in this region, but the cost is too high for general application. Hollow cathode lasers are available at several ultraviolet wavelengths, including a 224-nm silver–helium hollow cathode laser *(32),* and are much less expensive than frequency-doubled lasers, but presently these lasers are neither powerful enough nor reliable enough for routine use.

Raman Imaging

Raman imaging is either accomplished by taking individual spectra of an *x–y* grid or imaging a large sample area that is simultaneously exposed to the laser. In the latter case the Raman scattering is not sent through a spectrograph for wavelength dispersion, but through a tunable filter that selects only one wavelength. Next, the monochromatic scattering is imaged onto a two-dimensional array detector. A direct image of the sample areas that exhibit a Raman transition at the selected wavelength is obtained. Raman imaging is commonly accomplished with variable wavelength, tunable filters, such as liquid crystal tunable filters or acoutso–optical tunable filers *(33).* A heterogeneous sample can be quickly scanned to check for the presence of a particular compound or for the location and number of spatially distributed components. If enough images, each at a different wavelength, of a static sample are collected, full Raman spectra could be reconstructed to identify each component.

Summary

Raman spectroscopy has been reborn owing to improvements in lasers, optics, and detectors. Whereas Raman scattering was once considered an obscure technique, it is now thought, by many, to be just as useful as infrared analysis. Array detectors have resulted in greatly reduced measurement times not only because full spectra are collected without scanning, but also because they possess extreme sensitivity and have low noise. The incredible sensitivity of modern array detectors has allowed Raman spectroscopy to be used to detect compounds at part per million concentrations and to perform Raman analyses at advantageous wavelengths that were once nearly impossible to detect. Some of the newer applications, such as simultaneous collection of multiple spectra and Raman imaging, would be nearly impossible without two-dimensional array detectors. Array detectors are not solely responsible for the resurgence of Raman spectroscopy, but there can be no doubt of the tremendous impact array detectors have on Raman spectroscopy.

Literature Cited

1. Denton, M. B.; Denson, S. C.; Pommier, C. J. S. The Incredible Impact of Array Detectors on Raman Spectroscopy: Past, Present, and Future. Presentation at the Pittsburgh Conference for Analytical Chemistry and Applied Spectroscopy, Orlando, FL, March 9–14, 2003.

2. Giles, J. H.; Ridder, T. D.; Williams, R. H.; Jones, D. A.; Denton, M. B. *Anal. Chem.* **1998**, *70,* 663A–668A.
3. Sims, G. R. Principles of Charge-Transfer Detectors. In *Charge-Transfer Devices in Spectroscopy;* Sweedler, J. V., Ratzlaff, K. L., Denton, M. B., Eds.; VCH Publishers: New York, 1994; pp 9–58.
4. Pommier, C. J. S.; Walton, L. K.; Ridder, T. D.; Denton, M. B. *Array Detectors for Raman Spectroscopy;* John Wiley & Sons: Chichester, United Kingdom, 2002; Vol. 1.
5. Ingle, J. D.; Crouch, S. R. *Spectrochemical Analysis;* Prentice Hall: Englewood Cliffs, NJ, 1998.
6. Skoog, D. A.; Holler, F. J.; Nieman, T. A. *Principles of Instrumental Analysis,* 5th ed.; Saunders College Publishing: Philadelphia, 1998.
7. *Multichannel Image Detectors;* Talmi, Y., Ed.; American Chemical Society: Washington DC, 1983.
8. Chang, R. K.; Long, M. B. Optical Multichannel Detection. In *Light Scattering in Solids II;* Cardona, M., Guntherodt, G., Eds.; Springer–Verlag: Berlin, 1982; pp 179–205.
9. McCreery, R. L. Array Detectors for Multichannel Raman Spectroscopy. In *Charge-Transfer Devices in Spectroscopy;* Sweedler, J. V., Ratzlaff, K. L., Denton, M. B., Eds.; VCH Publishers: New York, 1994; pp 227–279.
10. Princeton Instruments. Technical Data Sheet: PDA 1024 Linear Array.
11. Boyle, W. S.; Smith, G. E. *Bell System Tech. J.* **1970**, *49,* 587.
12. Malina, E. G.; Nakhleh, M. B. *J. Chem. Educ.* **2003**, *80,* 691–698.
13. Giles, J. H.; Gilmore, D. A.; Denton, M. B. *J. Raman Spectrosc.* **1999**, *30,* 767–771.
14. Denton, M. B.; Sperline, R. P.; Giles, J. H.; Gilmore, D. A.; Pommier, C. J. S.; Downs, R. T. *Aust. J. Chem.* **2003**, *56,* 117–131.
15. Sims, G. R. Brief History of Charge-Transfer Devices. In *Charge–Transfer Devices in Spectroscopy;* Sweedler, J. V., Ratzlaff, K. L., Denton, M. B., Eds.; VCH Publishers: New York, 1994; pp 1–7.
16. Janesick, J.; Elliott, T. History and Advancements of Large Array Scientific CCD Imagers. In *Astronomical CCD Observing and Reduction Techniques;* Howell, Steve B., Ed.; Astronomical Society of the Pacific: San Francisco, 1992; Vol. 23.
17. *CRC Handbook of Chemistry and Physics,* 74th ed.; Lide, D. R., Ed.; CRC Press: Boca Raton, FL, 1993.
18. Chase, B. Arrays for Detection Beyond One Micron. In *Charge–Transfer Devices in Spectroscopy;* Sweedler, J. V., Ratzlaff, K. L., Denton, M. B., Eds.; VCH Publishers: New York, 1994; pp 109–131.
19. Chase, B.; Talmi, Y. *Applied Spectroscopy* **1991**, *45,* 929–931.
20. Engert, C.; Deckert, V.; Kiefer, W.; Umapathy, S.; Hamaguchi, H. *Applied Spectroscopy* **1994**, *48,* 933–936.
21. Barbillat, J.; da Silva, E. *Spectroc. Acta Pt. A-Molec. Biomolec. Spectr.* **1997**, *53,* 2411–2422.
22. Princeton Instruments. Techincal Data Sheet: "OMAV". *http://architect.wwwcomm.com/Uploads/Princeton/Documents/Datasheets/omav_1024-17ln.pdf* (accessed Oct 2006).
23. Rockwell Scientific Imaging Sensors: Hawaii 2.5 mm. *http://www.rsc.rockwell.com//imaging/hawaii1rg.html* (accessed Oct 2006).
24. Jerram, P.; Pool, P.; Bell, R.; Burt, D.; Bowring, S.; Spencer, S.; Hazelwood, M.; Moody, I.; Catlett, N.; Heyes, P. The LLLCCD: Low Light Imaging without the Need for an Intensifier. *http://www.ing.iac.es/~smt/LLLCCD/LLLCCD-SPIE4306A-201.pdf* (accessed Oct 2006).
25. Texas Instruments. Techincal Data Sheet: "TC253SPD 680x500 Pixel CCD Image Sensor". *http://focus.ti.com/lit/ds/symlink/tc253spd-30.pdf* (accessed Oct 2006).
26. Andor Technology. Electron Multiplying CCD. *http://www.andor-tech.com/2_new_emccd.htm* (accessed Sep 2006).
27. Roper Scientific. Techincal Data Sheet: "Cascade:650". *http://www.roperscientific.com/pdfs/datasheets/cascade/650.pdf* (accessed Oct 2006).
28. Atlus, G. Imager Labs, Irvine, CA, Personal communication, 2003.
29. Asher, S. A.; Munro, C. H.; Chi, Z. H. *Laser Focus World* **1997**, *33,* 99–109.
30. Princeton Instruments. Technical Data Sheet: "PI-MAX:1024UV". *http://content.piacton.com/Uploads/Princeton/Documents/Datasheets/pimax_1024_RevD3.pdf#search=%22PI-Max%20UV%201024%22* (accessed Oct 2006).
31. Marconi Applied Technologies. Technical Data Sheet: "CCD30-11 Back Illuminated High Performance CCD Sensor". *http://www.astrosurf.com/cavadore/CCD/Marconi/3011bi.pdf* (accessed Oct 2006).
32. Sparrow, M. C.; Jackovitz, J. F.; Munro, C. H.; Hug, W. F.; Asher, S. A. *Applied Spectroscopy* **2001**, *55,* 66–70.
33. Schaeberle, M. D.; Morris, H. R.; Turner, J. F.; Treado, P. J. *Anal. Chem.* **1999**, *71,* 175A–181A.